International Journal of Applied Science and Engineering
2012. 10, 4: 293-306

Studies of Chitosan at Different pH's in the Removal of Common Chlorinated Organics from Wastewater

Jih-Hsing Chang[a,*], Ching-Lung Chen[a], Amanda V. Ellis[b], and Cheng-Hung Tung[c]

[a] *Department of Environmental Engineering and Management, Chaoyang University of Technology, 168 Jifong E. Rd., Wufong District, Taichung, Taiwan, R.O.C.*
[b] *Centre for Nanoscale Science and Technology, School of Chemical and Physical Sciences, Flinders University, Sturt Rd, Bedford Park, Australia*
[c] *Department of Environmental Engineering, National Chung Hsing University, 250, Kuo Kuang Road, Taichung, Taiwan, R.O.C.*

Abstract: This work explores the use of chitosan as an adsorbent of common chlorinated organics in waste water, namely 4-chlorophenol and tetrachloroethylene. We use both isothermal adsorption equilibrium and dynamic adsorption experiments to describe the phenomena of adsorption at pH 4, 5, 6, 7 and 9. Results show that 4-chlorophenol is adsorbed the greatest at pH 6 while tetrachloroethylene is adsorbed the greatest at pH 4. The Langmuir constant b values range from 0.00003 to 0.00012 and 0.00001 to 0.00007 for 4-chlorophenol and tetrachloroethylene, respectively, and overall it appeared that the binding energy of 4-chlorophenol to chitosan is higher than that of tetrachloroethylene. Dynamic adsorption experiments show that the adsorption of 4-chlorophenol on chitosan follows a second order process while tetrachloroethylene follows a first order process, where the external mass transport coefficient of 4-chlorophenol and tetrachloroethylene ranged from 0.081 - 0.755 and 0.009 - 0.285, respectively. Additionally, the internal pore diffusion rate of 4-chlorophenol inside the micropores of chitosan is shown to be approximately 2.5 times that of tetrachloroethylene.

Keywords: Chitosan; adsorption; chlorinated organic; pH; CP-MAS ^{13}C NMR.

1. Introduction

The most commonly observed chlorinated organics in wastewater include 4-chlorophenol, trichloroethylene and tetrachloroethylene. In particular, 4-chlorophenol finds its way into wastewater through its use as a compound in the manufacture of pesticides, bactericides, wood preservatives and agricultural chemicals such as 2, 4-D and 2, 4, 5-T [1]. Similarly, trichloroethylene and tetrachloroethylene are used in many industries for their unique properties including solvent power, low flammability, chemical stability, low boiling point and high vapor pressure. Typical applications include dry-cleaning and degreasing, cleaning of metal parts and electronic components, cold cleaning, fumigants, paint strippers and textiles [2-4]. Consequently, inappropriate disposal or treatment of these chemicals can easily cause source water contamination.

* Corresponding author; e-mail: changjh@cyut.edu.tw
© 2012 Chaoyang University of Technology, ISSN 1727-2394
Received 19 June 2012
Revised 19 September 2012
Accepted 19 October 2012

Adsorption of organic contaminants on a variety of materials is frequently used in water treatment technologies. Examples of these adsorbents include chitosan [5], fly ash [6], and agricultural waste (olive kernel and corn cobs) [7]. All of which have proven to be very successful in water treatment due to their high adsorption capacity and environmental compatibility.

Chitosan (Figure 1, bottom) is a β-1, 4-linked polysaccharide that is obtained by partial deacetylation of chitin (Figure 1, top), a biopolymer which is the second most abundant natural polymer and exists widely in the shells of crustaceans and insects [8]. It is chitosan's abundance, non-toxicity, bio-compatibility, and bio-decomposability, in addition to its strength and porous structure, which make it ideal as an environmental remediation material. Furthermore, its chemical functional groups, -OH and -NH_2 (Figure 1, bottom), make it an ideal absorbent in the treatment of wastewater [9-10]. At low pH's the primary amines (-NH_2) are protonated and positively charged, and chitosan behaves as a water-soluble cationic polyelectrolyte. However, at pH's higher than pK_a ~ 6.3 the amines are deprotonated and chitosan becomes insoluble with gel forming characteristics [11]. In environmental engineering, chitosan has been used in removing heavy metals in wastewater [12] and the treatment of dyes [13-16]. In particular, chitosan has been found to adsorb approximately 1,940 to 1,945 g kg^{-1} of an anionic dye under acidic conditions as well as effectively removing up to 99% of the dyes chromaticity [10]. The adsorption mechanism has been described by a pseudo-second order dynamic model [15, 17-19]. However, very little to date has been reported on the adsorption mechanism of chlorinated organic contaminants on chitosan and it is here we present this work. Chitosan was investigated as an adsorbent for 4-chlorophenol and tetrachloroethylene and a series of isothermal adsorption equilibrium and dynamic adsorption experiments were carried out at various concentrations and pH's. In addition, the related adsorption equilibrium and dynamic adsorption parameters were obtained.

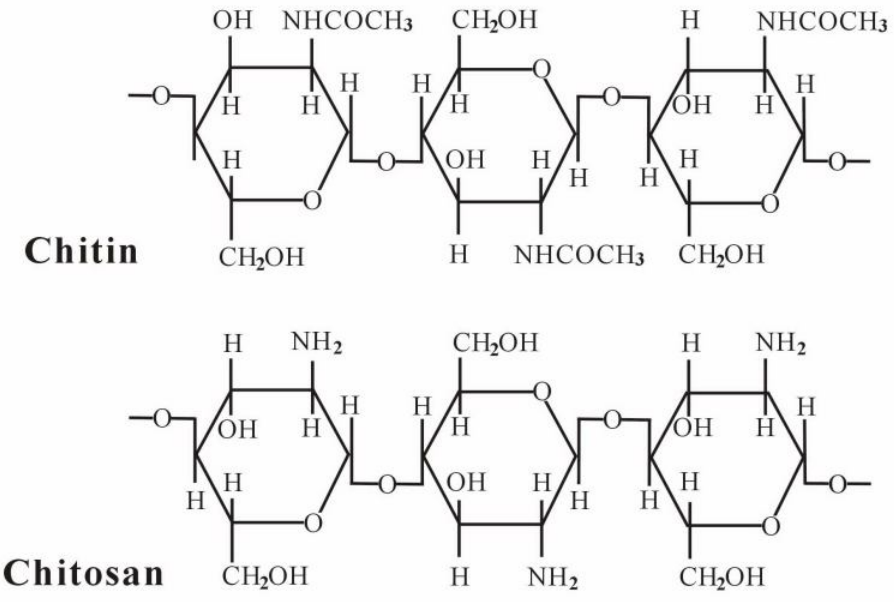

Figure 1. Structural formula of chitin and chitosan

2. Material and methods

Commercially available chitosan was provided by Cheng-Li Corporation and is the deacetylated form (90%) of chitin extracted from shrimp shells and has a specific surface area of 10.3 $m^2 g^{-1}$. Chitosan powder with diameters in the range of 100 to 120 mesh were selected using an appropriate sieve. The target pollutants were 4-chlorophenol (Fluka, ≥ 98%) and tetrachloroethylene (J.T. Baker, ≥ 99%). Reagents used for adjusting the pH of the target pollutants were 0.05 M sulfuric acid (PEF, 97%) and 0.5 M sodium hydroxide (RDH, 98%). Hexane (J.T, Baker, 95%) was used as an extracting agent. The extraction procedures were referred to Wang, 1997. For the treatment of chitosan at pH 4, 5, 6, 7 and 9 aqueous solutions of 0.01 M acetic acid (RDH, 99.8%) and 0.5 M sodium hydroxide (RDH, 98%) were used, respectively.

2.1. Treatment of chitosan at various pH's

Chitosan (1 g) was added to deionized water (100 mL) and the pH's of the suspension were controlled through the addition of either 0.01 M acetic acid or 0.5 M sodium hydroxide to pH's of 4, 5, 6, 7 or 9. The suspensions were then left for 4.5 h with constant stirring at room temperature. After 4.5 h the suspension was filtered off under vacuum and the chitosan washed with deionized water and then dried in a desiccator.

2.2. Specific surface area of chitosan

A Micromeritics Instrument Corporation ASAP 2020 analyzer was used to measure the specific surface area and pore size of the dried chitosan after treatment at pH 4, 5, 6, 7 and 9 at 77 K using N_2 as the adsorption and desorption gas. Each measurement was repeated three times.

2.3. CP-MAS 13C nuclear magnetic resonance (NMR) spectroscopy

Samples of pristine chitosan and chitosan that had been previously treated at pH 4,5,6,7 and 9 (0.5~1.0 g) were added into a NMR tube for analysis, with an inner diameter of 10 mm and a height of 4 cm. A CP-MAS ^{13}C NMR spectrometer (Bruker MSL-2000 NMR) was used to measure the types of carbon in the chitosan after treatment at different pH's. The spectrum frequency range of the spectrometer was 50.33 MHz with a delay time of 1 ms, a cycle time of 1 s and a magic angle speed of 3.5 kHz. The chemical shift (ppm) can be divided into 5 regions; 0-50 ppm (alkyl carbon), 50-90 ppm (hydrocarbons such as alcohol, ether or fat), 90-110 ppm (aldehyde carbon), 110-160 ppm (aromatic carbon) and 160-190 ppm (carboxyl carbon) [20]. These zones were subsequently integrated in order to find the percentages of the respective carbon types in each sample.

2.4. Batch isothermal adsorption equilibrium experiments

For batch isothermal adsorption equilibrium experiments solutions of 4-chlorophenol were made up in water to concentrations of 0.04 Cs, 0.06 Cs, 0.08 Cs, 0.1 Cs, 0.2 Cs, 0.3 Cs, 0.4 Cs, 0.5 Cs, where Cs is the saturated solubility of 4-chlorophenol in water (Cs = 27,000 mg L^{-1}). Similarly, solutions of tetrachloroethylene were made up in water to concentrations of 0.05 Cs, 0.1 Cs, 0.2 Cs, 0.3 Cs, 0.4 Cs, 0.5 Cs, 0.6 Cs, 0.7 Cs, 0.8 Cs, where Cs is the saturated solubility of tetrachloroethylene in water (Cs = 150 mg L^{-1}). All solution pH's were controlled through the addition of either 0.05 M sulfuric acid or 0.5 M sodium hydroxide to pH's of 4, 5, 6, 7 and 9.

Batch isothermal adsorption experiments were then performed at pH's 4, 6, 7 and 9

for 4-chorophenol and 4, 5, 6, 7 and 9 for tetrachloroethylene. Chitosan (0.5 g) and target pollutant solutions (12.5 mL) were added to a glass tube and placed on a shaker (Deng Yug) for 48 h. The sample was then centrifuged (Hettich Zentrifugen EBA 12) at 3000 rpm for 10 min and the clear upper solution (1 mL) was then removed and added to hexane (10 mL). This mixture was then centrifuged for 10 min after which the upper hexane layer containing the extracted organochlorines was removed and placed into a gas chromatography instrument with an electronic detector (GC/ECD; Varian CP3800). Isothermal adsorption equilibrium profiles were calculated from this data.

2.5. Dynamic adsorption experiments

In order to perform dynamic adsorption experiments a mixing/agitator set-up (Figure 2(A)) and continuous flow fixed bed (Figure 2(B)) were used. Solutions of 4-chlorophenol (500 mg L^{-1}) and tetrachloroethylene (80 mg L^{-1}) at pH's of 4, 5, 6, 7 and 9 were used.

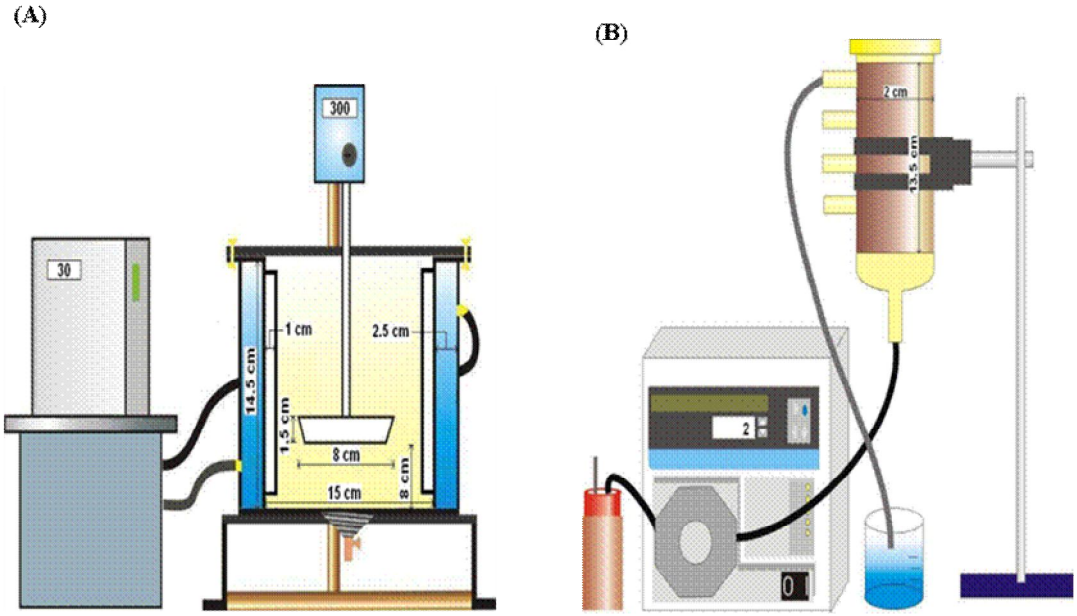

Figure 2. (A) Dynamic adsorption mixing/agitator set-up and (B) continuous flow fixed bed for adsorption of chlorinated organic pollutants on chitosan

2.5.1. Batch dynamic contact time experiments

Each experiment required chitosan (50 g) and a volume of each concentration of the target pollutant (2.7 L) to be loaded into a mixing/agitator tank. The mixing/agitation tank (Figure 2(A)) was constructed with a diameter and height of 15 cm and within the tank body eight baffles were installed on the peripherals with even spacing. The agitator vane was made of Teflon with a diameter of 8 cm. A variable speed motor (Ika-Werke) was used to drive the vane at 300 rpm and an isothermal compact refrigerated circulating bath (Julabo F30-C) was used to maintain the solution temperature at 303 K. At various time intervals, starting at t = 0, samples (5 mL) were removed and extracted in hexane as per section 2.4 and then analyzed using GC/ECD.

2.5.2. Continuous flow fixed bed experiments

The fixed bed consisted of a glass tube

with an inner diameter of 2 cm (Figure 2(B)) a plug of glass wool was used to prevent the chitosan from coming out of the tube. An evenly distributed bed of chitosan (14 g) was added to the glass tube at a height of approximately 13.5 cm. Each of the target pollutant concentrations and various pH's were flowed up through the bed using a quantitative motor (Cole-Parmer 7524-40) at an input flow rate of 2 mL min^{-1}. At various time intervals, starting at t = 0, samples (0.5 mL) were removed and extracted in hexane as per section 2.4 and then analyzed using GC/ECD.

3. Results and discussion

3.1. Characterization of chitosan after treatment at different pH's

Chitosan is highly affected by the pH of the environment this in turn leads to the change in its properties such as specific surface area and average pore size distribution. Here we discuss how these changes were monitored using specific surface area analysis, pore size analysis and CP-MAS ^{13}C NMR spectroscopy.

3.1.1. Specific surface area and pore size analysis

The specific surface area and average pore size distribution of chitosan after treatment at different pH's (from 4 to 9) were measured which distributed around 10.3 - 19.7 m^2 g^{-1} and 67.5 - 69.1 Å, respectively. At pH 4 chitosan has the largest average specific surface area and average pore size, at 19.7 m^2 g^{-1} and 69.1 Å, respectively. This larger specific area with low pH has previously been reported to be due to the gradual dissolution of the chitosan to a protonated water-soluble cationic polyelectrolyte, especially at pH's lower than 5.5 [18]. At pH 9 the chitosan is in the gel state with a minimum specific surface area of 10.5 m^2 g^{-1}, however the average pore size remains unchanged at 69.1 Å.

3.1.2. CP-MAS ^{13}C NMR analysis

Figure 3(A-F) show the CP-MAS ^{13}C NMR spectra of chitosan after treatment at different pH's, wherein A, B, C, D, E and F represent pristine chitosan, pH 4, pH 5, pH 6, pH 7 and pH 9, respectively. The percentage carbon types within each sample were computed (not shown here). Overall, as expected, there is no noticeable change in the chemical make-up of the chitosan at varying pH other than it appears that the O-alkyl content is slightly higher at lower pH values. This could be due to the reduced steric hindrance of the CH_2OH groups in the chitosan (Figure 1, bottom) in the more extended cationic polyelectrolyte form present at lower pH.

3.2. Isothermal adsorption equilibrium experiments

During the isothermal adsorption equilibrium experiments chitosan remains in the target pollutant solution for 48 h to reach equilibrium after which the equilibrium concentration C_e (mg L^{-1}) of the target pollutant is then analyzed and the adsorption capacity q_e (mg kg^{-1}) is calculated using Equation 1.

$$q_e = \frac{(C_o - C_e) \times V}{W} \quad (1)$$

Where q_e is the amount of adsorbed target pollutant at equilibrium per unit chitosan (mg kg^{-1}), C_o is the initial concentration of the target pollutant solution (mg L^{-1}), C_e is the equilibrium concentration of the target pollutant solution (mg L^{-1}), V is the volume of target pollutant solution (L) and W is the weight of chitosan (kg).

Figure 4(A and B) show the isothermal equilibrium adsorption profiles of

4-chlorophenol and tetrachloroethylene, respectively, at different pH's. These profiles correspond to a Langmuir isothermal equilibrium adsorption model (Equation 2) with R^2 values of 0.898~0.907 and 0.898~0.940 for 4-chlorophenol and tetrachloroethylene , respectively.

$$q_e = \frac{QbC_e}{1+bC_e} \quad (2)$$

Where q_e is the amount of adsorbed target pollutant at equilibrium per unit chitosan (mg kg^{-1}), Q is the maximum amount of adsorbed target pollutant per unit chitosan (mg kg^{-1}), C_e is the equilibrium concentration of the target pollutant solution (mg L^{-1}) and b is the Langmuir constant.

Figure 4(A) shows that the adsorption capacity of chitosan for 4-chlorophenol increases with increasing equilibrium concentration and that this adsorption capacity is effected by the pH such that the amount of 4-chlorophenol adsorbed increases in the order of pH 6> pH 4> pH 7> pH 9. Given that the pK_a of chitosan's amine groups is approximately 6.3 it is expected that there will be protonation of the amines ($-NH_3^+$) [18], as well as water-solubility of this biopolymer at pH 6. Additionally, the degree of chitosan ionization decreases from 1.0 to 0.5 as pH increases from 4.0 to 6.2 [21]. This means that the amino groups become less charged as pH increases. As a result, it may be expected that there would be less bonding of the 4-chlorophenol at pH 6 than pH 4. However, since the charge density of the chitosan molecule is reduced by almost 50% as the pH approaches 6.2 from 4.5, the polymer chains become less extended with a smaller radius of gyration [22], and are still water soluble. This potentially results in a higher diffusion coefficient for chitosan chains at pH 6.2 and consequently binding more 4-chorophenol. Figure 4(B) shows the isothermal adsorption equilibrium profiles of tetrachloroethylene at different pH's. Again the adsorption capacity of chitosan for the pollutant increases with increasing equilibrium concentration. However, this time the adsorption capacity is effected by the pH such that the amount of tetrachloroethylene adsorbed increases in the order of pH 4> pH 5> pH 6> pH 7> pH 9. Here the reason that the tetrachloroethylene is not adsorbed the greatest at pH 6 is that in addition to water-solubility there is also hydrogen bonding of the target pollutant to the chitosan. Given that the dissociation constant (pK_a) of 4-chlorophenol is 9.38 at 25 °C [23] 4-chorophenol will be protonated and in its molecular state. The presence of –OH groups on the 4-chorophenol and the –OH groups on the chitosan further enables adsorption of the pollutant onto the chitosan through hydrogen bonding. This hydrogen bonding cannot occur with tetrachloroethylene.

The Langmuir isothermal equilibrium adsorption model parameters of 4-chlorophenol and tetrachloroethylene on chitosan are calculated. The Langmuir constant b values range from 0.00003 to 0.00012 and 0.00001 to 0.00007 for 4-chlorophenol and tetrachloroethylene, respectively. The b values represent the binding energy of adsorption and these increase with increasing binding energy of adsorption. Thus for 4-chlorophenol the binding energy increases from pH 9 to pH 6 but then decreases at pH 4. Clearly the adsorption binding energies are lower for tetracholorethylene on chitosan than 4-chlorophenol.

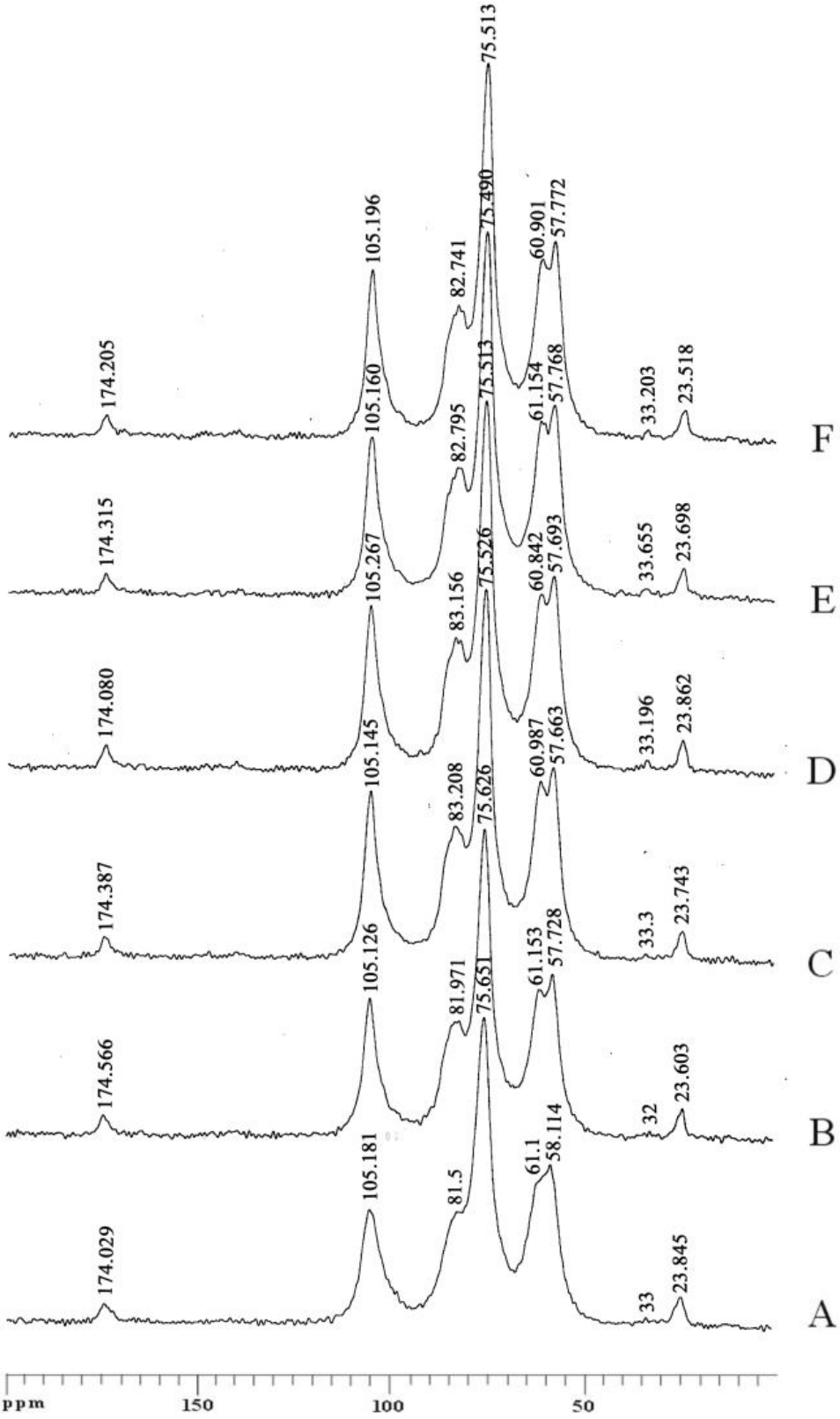

Figure 3. CP-MAS ^{13}C NMR spectra of chitosan after treatment at different pH's, wherein A, B, C, D, E and F represent pristine chitosan, pH 4, pH 5, pH 6, pH 7 and pH 9, respectively

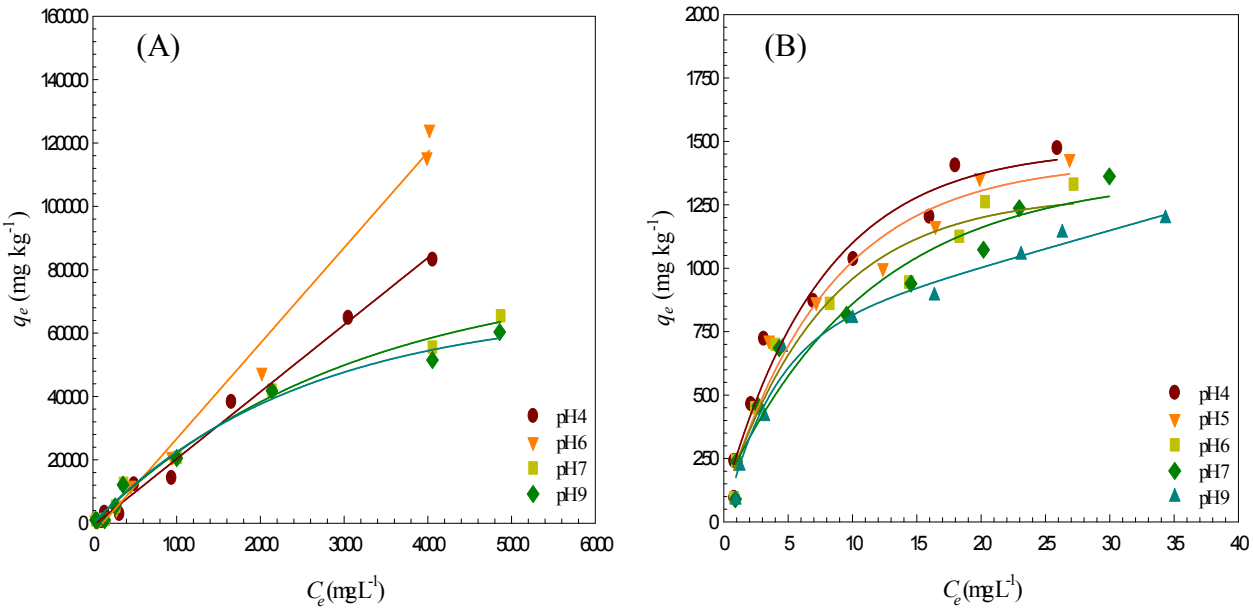

Figure 4. Isothermal adsorption profiles of (A) 4-chlorophenol and (B) tetrachloroethylene on chitosan at different pH's.

3.3. Dynamic adsorption experiments

Based on the dynamic adsorption results (Figure 5(A and B)) the dynamic phenomena of 4-chlorophenol and tetrachloroethylene adsorption on chitosan were investigated. This involved studying the reaction order of adsorption (Figure 6), external mass transport coefficients of the external surface and the diffusion rates within the pores (Figure 7).

3.3.1. Order of reaction

3.3.1.1. First-order reaction

A first order reaction rate is one in which the reaction rate is proportional to the concentration of the target pollutant in solution, and is given by Equation 3 [24].

$$\ln C_t = \ln C_o - kt \quad (3)$$

Where C_t is the target pollutant concentration per unit volume (mg L^{-1}), C_o is the initial pollutant concentration (mg L^{-1}), k is the reaction rate constant (min^{-1}), t is the time (min). If the data of the adsorption experiments follows a first order reaction then a plot of lnC_t versus t will result in a linear regression line with a slope k.

3.3.1.2. Second-order reaction

A second order reaction rate is one in which the reaction rate is proportional to square of the concentration of the target pollutant in solution, and is given by Equation 4.

$$\frac{1}{C_t} = \frac{1}{C_o} + kt \quad (4)$$

Thus if the adsorption data follows a second order reaction then a plot of 1 / C_t versus t will result in a linear regression line with a slope of k. Profiles of the dynamic adsorption of 4-chlorophenol and tetrachloroethylene versus time are shown in Figure 5(A and B). The reduction in concentration for both 4-chorophenol and tetrachloroethylene shows an exponential decay at all pH's. For 4-chlorophenol the adsorption occurs most rapidly over the first

60 min to 80 min with the adsorption at pH 7 and pH 9 being the fastest (Figure 5(B)). After 80 min the adsorption remains constant at all pH's which indicates the binding sites on the chitosan are fully saturated with the 4-chlorophenol after this time. For tetrachloroethylene the adsorption onto chitosan is much quicker and occurs within the first 20 min at all pH's after which the chitosan binding sites are saturated (Figure 5(B)). We summarized the rate constants k and R^2 of the regression fitting for both a first and second order reaction (not shown here). From the R^2 values we can predict that the adsorption of 4-chlorophenol is most likely a second order reaction. Furthermore, for the adsorption of 4-chlorophenol on chitosan the fastest reaction rate is that at pH 6 (3.699×10^{-5} L mol^{-1} min^{-1}) and follows a second order process while for tetrachloroethylene the fastest reaction rate occurs pH 4 (0.066 min^{-1}) and follows a first order process.

3.3.2. External mass transport coefficient

The mass transport of an adsorbate (target pollutant) on the external surface of an adsorption material (chitosan) is given by Equation 5 [9]:

$$\left[\frac{d\left(C_t/C_o\right)}{dt}\right]_{t=0} = -k_s S_m \quad (5)$$

Where C_t is the target pollutant concentration per unit volume (mg L^{-1}), C_o is the initial target pollutant concentration per unit volume (mg L^{-1}), k_s is the mass transport coefficient of the external surface (m s^{-1}), s_m is the maximal particulate external surface area of the target pollutant per unit volume (m^2 L^{-1}). A plot of C_t/C_o versus t (min) results in a linear regression line by then using a forward differential the first order derivative value at t = 0 can be calculated and the k_sS_m value can be obtained. The S_m values can be obtained from Equation 6 (the particulate external surface area of target pollutant in solution).

$$S_m = \frac{6M_m}{d_p \rho_p} \quad (6)$$

Where M_m is the mass of target pollutant per unit solution (kg m^{-3}), d_p is the average particulate size (μm), ρ_p is the volume density of the chitosan (kg m^{-3}). Once S_m has been established this is then substituted into Equation 5 and k_s (mass transport coefficient of external surface) is calculated.

From Figure 6(A and B), where C_t/C_o is plotted versus t (min) for the dynamic adsorption of 4-chlorophenol and tetrachloroethylene, respectively, the mass transport coefficient of the external surface can be calculated. Typical k_s values in literature on the mass transport of dyes with chitosan are around 1.374×10^{-5} m s^{-1} [9]. The values reported in this work are much higher ranging from 0.081 m s^{-1} to 0.755 m s^{-1} for 4-chlorophenol and 0.009 m s^{-1} to 0.285 m s^{-1} for tetrachloroethylene with no apparent trend in the mass transport of either pollutant at different pH's. We account for this increased mass transport as a result of the lower molecular weights of 4-chlorophenol (128.56 g mol^{-1}) and tetrachloroethylene (165.9 g mol^{-1}) compared to those of the dyes used in previous studies (350.3~622.6 g mol^{-1}) [25].

3.3.3. Diffusion rate parameter within the pore

When the concentration gradient diffuses in a single direction along the x-axis the basic differential equation of Fick's second law which is set to individual boundary conditions is often very complicated to solve. Thus Equation 7 is often used [13].

$$q_t = k_d t^{1/2} \quad (7)$$

Where $t^{1/2}$ (min) is the square root of time and used to describe the pore diffusion behavior inside the chitosan particulate, q_e is

the amount of adsorbed target pollutant per unit chitosan mass (mg kg^{-1}) and k_d is the diffusion constant within the chitosan particulate (mg kg^{-1} $min^{-1/2}$). By plotting q_t versus $t^{1/2}$ the linear regression line gives rise to a slope k_d. This k_d value can then be used to assess the internal diffusion behavior of the target pollutant within the chitosan.

Figure 7(A and B) show the breakthrough profiles of 4-chlorophenol and tetrachloroethylene, respectively on chitosan at different pH's. These plots can be divided into 3 regions of interest. (1) the momentary adsorption step (k_p, 1) which arises from the chitosan external surface and some of the surfaces of the macropores. This diffusion behaviour is very rapid and therefore cannot be calculated accurately. (2) is the asymptotic adsorption step (k_p, 2) in which the target pollutant undergoes internal diffusion within the macropores of the chitosan. (3) is the equilibrium step (k_p, 3) and this is mainly based on the internal diffusion of the target pollutant within the microporous chitosan structure.

For 4-chlorophenol (Figure 7(A)), the k_p, 1 occurs within the first 5 min ($t^{1/2}$ = 2.24); k_p, 2 occurs between 5 to 60 min ($t^{1/2}$ = 2.24 to 7.75) and k_p, 3 occurs between 60 to 300 min ($t^{1/2}$ = 7.75 to 17.32). However, for tetrachloroethylene k_p, 1 again occurs in the first 5 min ($t^{1/2}$ = 2.24); k_p, 2 occurs over a slightly shorter time between 5 to 20 min ($t^{1/2}$ = 2.24 to 4.47) and k_p, 3 occurs again slightly shorter between 20 to 60 min ($t^{1/2}$ = 4.47 to 7.75). This data suggests that 4-chlorophenol has a faster diffusion rate within the chitosan pores than tetrachloroethylene. From Figure 7(A and B) the *kp*, 2 and *kp*, 3 for both 4-chlorophenol and tetrachloroethylene were calculated. It is noticed that k_p, 2 of 4-chlorophenol has a diffusion rate 2.5 times faster than that of tetrachloroethylene, presumably due to its lower molecular weight.

3.4. Continuous flow fixed bed experiments

To calculate the target pollutant adsorption capacity of a continuous flow chitosan fixed bed Equation 8 was used (Larry, 1982) [26].

$$S_{\max} = C_o\left(V_E - V_B\right) \tag{8}$$

Where $S_{\max}$ is the maximum adsorption amount of a fixed bed (mg g^{-1}), C_o: the initial concentration of the target pollutant per unit volume (mg L^{-1}) and $V_E - V_B$ is the processed wastewater volume (mL) between penetration and saturation.

The $S_{\max}$ calculated from Equation 8 for the amount of 4-chlorophenol and tetrachloroethylene adsorbed on a chitosan fixed bed at different pH's. At pH 6 4-chlorophenol has the maximum adsorption on chitosan at 1,415 mg kg^{-1} while tetrachloroethylene has a maximum adsorption amount of 524 mg kg^{-1} at pH 4. This corroborates well with the results from the isothermal adsorption equilibrium experiment Figure 5(A) suggesting again that the protonated chitosan is more effective at removing 4-chorophenol than tetrachloroethylene.

4. Conclusions

Here we describe the adsorption of 4-chlorophenol and tetrachloroethylene on chitosan at pH 4, 5, 6, 7, and 9. Our findings show that chitosan has a higher specific surface at pH 4 (19.7 m^2/g) which decreases down to 10.5 m^2/g at pH 9 while the pore size remains essentially the same. By using ^{13}CP-MAS NMR spectroscopy, here is little change in the functional groups with pH a slight increase in the O-alkyl groups at low pH may indicate that the extended form of the protonated cationic electrolyte is present at these lower pH's.

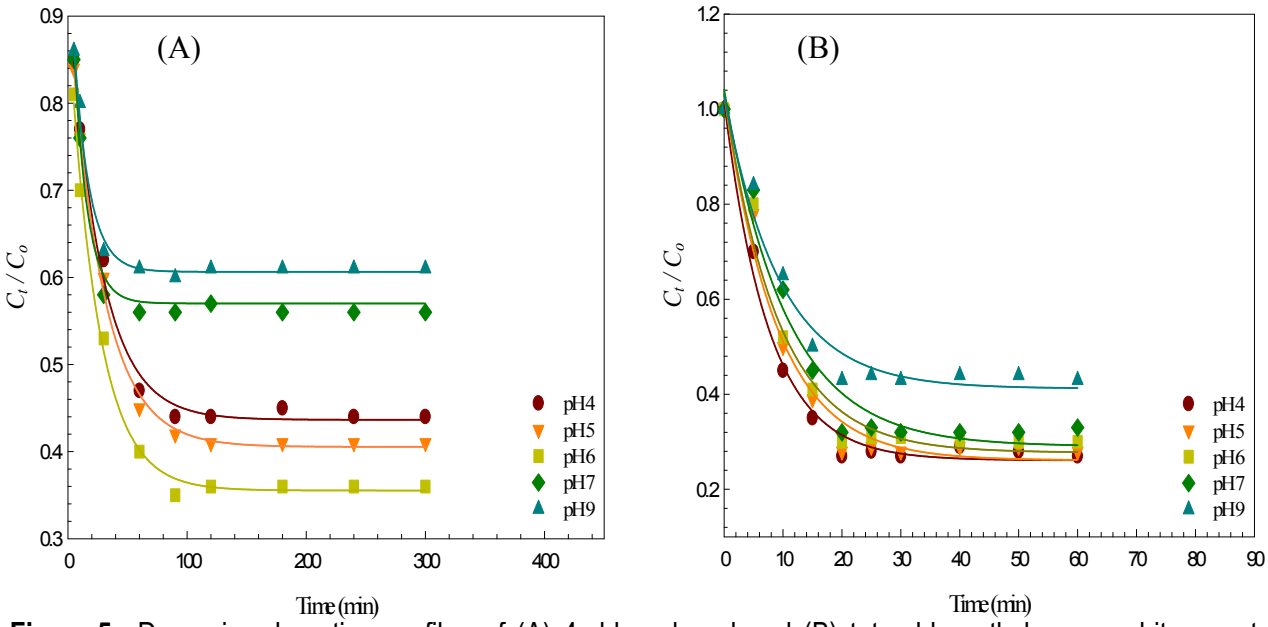

Figure 5. Dynamic adsorption profiles of (A) 4-chlorophenol and (B) tetrachloroethylene on chitosan at different pH's

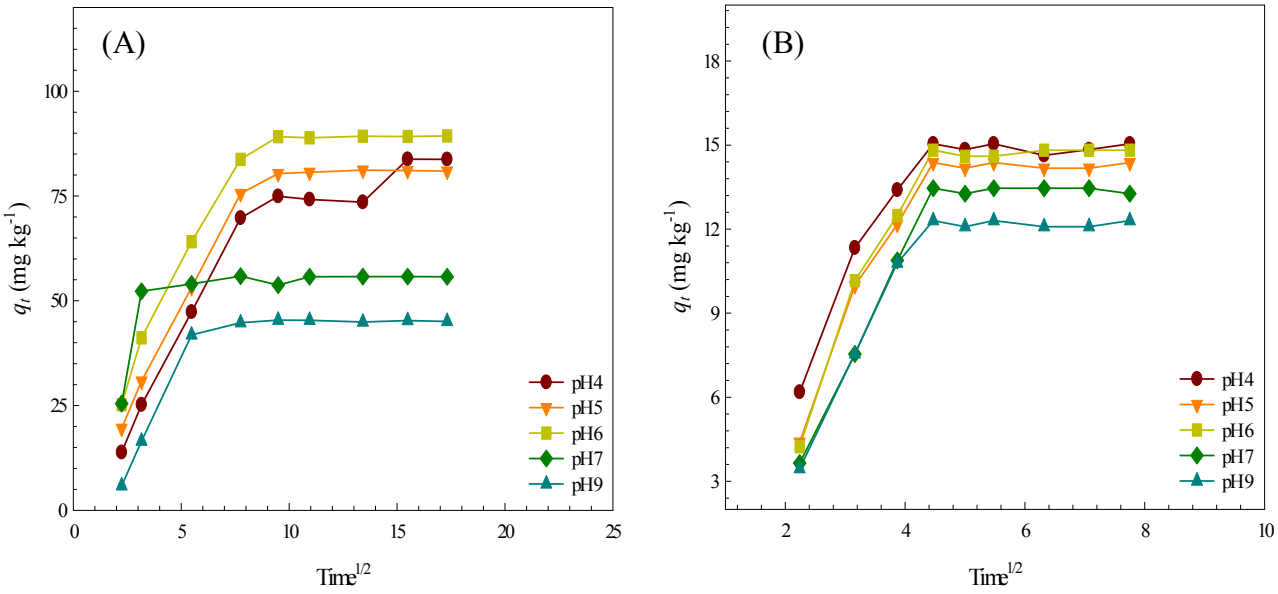

Figure 6. Profiles of internal pore diffusion speed (q_t) and the square root of time ($t^{1/2}$) for the adsorption of (A) 4-chlorophenol and (B) tetrachloroethylene on chitosan at different pH's

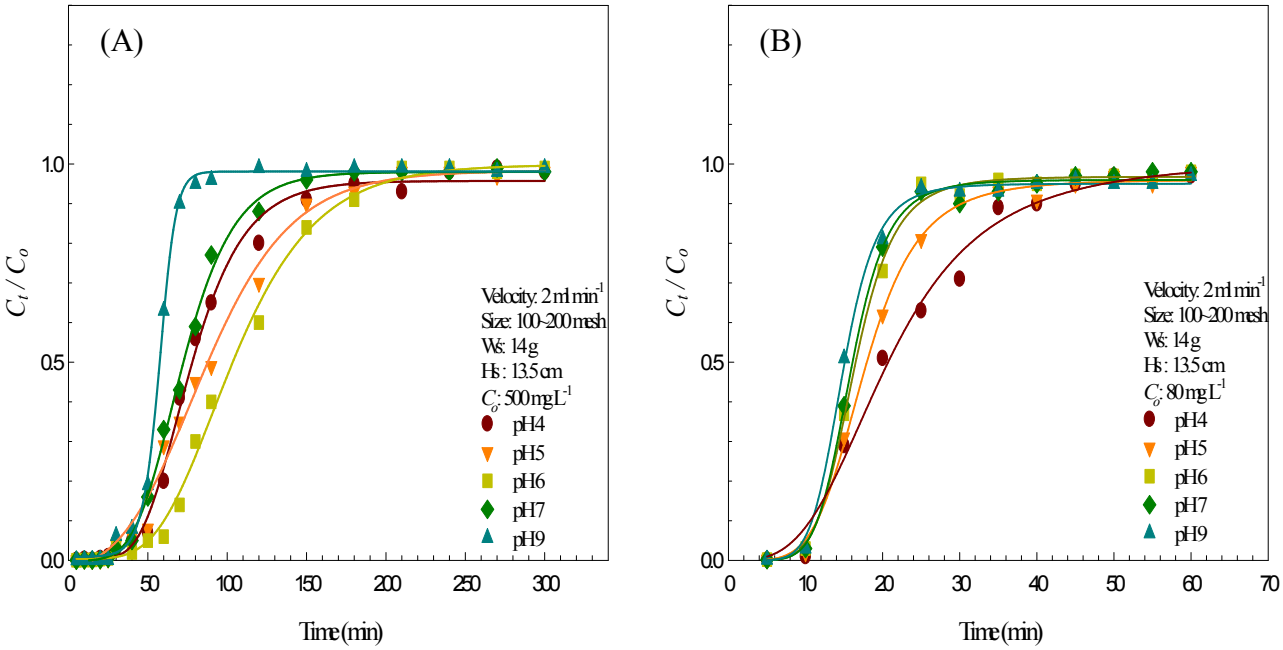

Figure 7. The breakthrough profiles of (A) 4-chlorophenol and (B) tetrachloroethylene on chitosan at different pH's

We show that the amount of 4-chlorophenol adsorbed onto chitosan at different pH's decreased in the order of pH 6> pH 4> pH 7> pH 9, which could be attributed to a combination of both hydrogen bonding of the protonated 4-chlorophenol and the smaller radius of gyration of chitosan at pH 6. Furthermore we found that the adsorption amount of tetrachloroethylene by chitosan at different pH's was pH 4> pH 5> pH 6> pH 7> pH 9. Here there is no hydrogen bonding between tetrachloroethylene and the chitosan and thus the order is different than for 4-chlorophenol. Dynamic adsorption experiments show that the reaction order of the adsorption of 4-chlorophenol on chitosan follows a second order reaction (R^2 value 0.901 ~ 0.982) while tetrachloroethylene follows a first order reaction (R^2 value 0.811 ~ 0.944), where the external mass transport coefficient of 4-chlorophenol and tetrachloroethylene ranged from 0.081 - 0.755 and 0.009 - 0.285, respectively. Additionally, the internal pore diffusion rate of 4-chlorophenol is shown to be approximately 2.5 times that of tetrachloroethylene.

Acknowledgments

This study is supported by the project research fund of National Science Council (Project no.: NSC92-2622-E-324-002-CC3), we would like to express our acknowledgment.

References

[1] Wang, Y. H. 1997. "*Environmental pollution and agricultural chemical on the soil*". Ming-Wen. Taiwan.

[2] Tsai, C. H. and Kuo, C. L. 1988. Investigation of underground water source polluted by alkyl-chloro compound in northern Taiwan. *Thesis collection on underground water source forum*.

[3] Tsai, W. T. 1992. Toxicity and metabolism mechanism of chlorinated

organic solvent. *J. industrial solution prevention*. 11: 175-187.
[4] Cookson, J. T. 1995. "*Bioremediation Engineering: Design and Application*". McGraw-Hill. New York.
[5] Zhang, X. and Bai, R. 2003. Mechanisms and kinetics of humic acid adsorption onto chitosan-coated granules. *J. Colloid Interface Sci*. 264: 30-38.
[6] Wang, S. and Zhu, Z. H. 2007. Humic acid adsorption on fly ash and its derived unburned. *J. Colloid Interface Sci*. 315: 41-46.
[7] Ioannidou, O. A., Zabaniotou, A. A., Stavropoulos, G. G., Islam, M. A., and Albanis, T. A. 2010. Preparation of activated carbons from agricultural residues for pesticide adsorption. *Chemosphere*. 80: 1328-1336.
[8] Yoshida, H., Okamoto A., and Kataoka T. 1993. Adsorption of acid dye on cross-linked chitosan fibers: equilibria. *Chem. Eng. Sci*. 48: 2267-2272.
[9] Wu, F. C., Chang, M. Y., and Tseng, J. L. 1996. The adsorption on dye solution by chitosan-isothermal equilibrium, dynamics and fixed bed adsorption. *Technical Journal*. 11: 501-511.
[10] Chiou, M. S., Ho, P. Y., and Li, H. Y. 2004. Adsorption of anionic dyes in acid solutions using chemically cross-linked chitosan beads. *Dyes pigm*. 60: 69-84.
[11] Luo, X., Berlin, D. L., Betz, J., Payne, G. E., Bentley, W. E., and Rubloff, G. W. 2010. In situ generation of pH gradients in microfluidic devices for biofabrication of freestanding, semi-permeable chitosan membranes. *Lab Chip*. 10: 59-65.
[12] Kumar, M. N. V. R. 2000. A review of chitin and chitosan applications. *React. Funct. Polym*. 46: 1-27.
[13] Wu, F. C., Tseng, R. L., and Juang, R. S. 2000. Comparative adsorption of metal and dye on flake- and bead-types of chitosan prepared from fishery wastes. *J. Hazard. Mater*. 73: 63-75.
[14] Wu, F. C., Tseng, R. L., and Juang, R. S. 2000. Kinetic modeling of liquid-phase adsorption of reactive dyes and metal ions on chitosan. *Water Res*. 35: 613-618.
[15] Annadurai, G., Ling, L. Y., and Lee, J. F. 2008. Adsorption of reactive dye from an aqueous solution by chitosan: isotherm, kinetic and thermodynamic analysis. *J. Hazard. Mater*. 152: 337-346.
[16] Chiou, M. S. and Li, H. Y. 2003. Adsorption behavior of reactive dye in aqueous solution on chemical cross-linked chitosan beads. *Chemosphere*. 50: 1095-1105.
[17] Annadurai, G. and Krishnan, M. R. V. 1997. Adsorption of acid dye from aqueous solution by chitin: Batch kinetic studies. *Indian J. Chem. Technol*. 4: 213-222.
[18] Chiou, M. S. and Li, H. Y. 2002. Equilibrium and kinetic modeling of adsorption of reactive dye on cross-linked chitosan beads. *J. Hazard. Mater*. 93: 233-248.
[19] Chatterjee, S., Chatterjee, B. P., Das, A. R., and Guha, A.K. 2005. Adsorption of a model anionic dye, eosin Y, from aqueous solution by chitosan hydrobeads. *J. Colloid Interface Sci*. 288: 30-35.
[20] Perminova, I. V., Grechishcheva, N. Y., and Petrosyam, V. S. 1999. Relationships between structure and bing affinity of humic substance for polycyclic aromatic hydrocarbons: relevance of molecukar descriptors. *Environ. Sci. Technol*. 33: 3781-3787.
[21] Ikeda, S., Kumagai, H., Sakiyama, T., Chu, C. H., and Nakamura, K. 1995. Method for analyzing pH-sensitive swelling of amphoteric hydrogels—Application to a

polyelectrolyte complex gel prepared from xanthan and chitosan. *Biosci. Biotechnol. Biochem*. 59: 1422-1427.
[22] Argin-Soysala, S., Kofinas, P., and Loa, Y. M. 2009. Effect of complexation conditions on xanthan–chitosan polyelectrolyte complex gels. *Food Hydrocolloids*. 23: 202-209.
[23] Slater, B., McCormack, A., Avdeef, A., and Comer, J.E.A. 1994. Comparison of partition coefficients determined by shake-flask, HPLC, and potentiometric methods. *Pharm. Sci.* 83: 1280-1283.
[24] William W. N. and Lisa A.C. 2001. "*Environmental Engineering Science*". John Wiley & Sons. New York.
[25] McKay, G., Wong, Y. C., Szeto, Y. S., and Cheung, W. H. 2004. Adsorption of acid dyes on chitosan ─ equilibrium isotherm analyses. *Water Res*.39: 695-704.
[26] Larry D. B., Joseph F. J., and Barron L.W. 1982. "*Process chemistry for water and wastewater treatment, in: Michaels, A.E., Removal of Soluble Organic Materials from Wastewater by Carbon Adsorption*". Prentice-Hall Inc. New Jersey. 389-431.